Journal of Alloys and Compounds 509 (2011) 10050–10054

Contents lists available at ScienceDirect

Journal of Alloys and Compounds

journal homepage: www.elsevier.com/locate/jallcom

Surfactant assisted electrodeposition of MnO_2 thin films: Improved supercapacitive properties

D.P. Dubal[a,b], W.B. Kim[b], C.D. Lokhande[a,*]

[a] Thin Film Physics Laboratory, Department of Physics, Shivaji University, Kolhapur 416004 (M.S.), India
[b] School of Materials Science and Engineering, Gwangju Institute of Science and Technology, 261 Cheomdan-gwagiro, Buk-gu, Gwangju 500-712, Republic of Korea

ARTICLE INFO

Article history:
Received 6 October 2010
Received in revised form 1 August 2011
Accepted 6 August 2011
Available online 12 August 2011

Keywords:
Amorphous materials
Thin films
Chemical synthesis
Energy storage

ABSTRACT

In order to obtain a high specific capacitance, MnO_2 thin films have been electrodeposited in the presence of a neutral surfactant (Triton X-100). These films were further characterized by means of X-ray diffraction (XRD), Fourier transform infrared (FTIR) spectroscopy, field emission scanning electron microscopy (FESEM) and contact angle measurement. The XRD studies revealed that the electrodeposited MnO_2 films are amorphous and addition of Triton X-100 does not change its amorphous nature. The electrodeposited films of MnO_2 in the presence of the Triton X-100 possess greater porosity and hence greater surface area in relation to the films prepared in the absence of the surfactant. Wettability test showed that the MnO_2 film becomes superhydrophilic from hydrophilic due to Triton X-100. Supercapacitance properties of MnO_2 thin films studied by cyclic voltammetry, galvanostatic charge–discharge cycling and impedance spectroscopy showed maximum supercapacitance for MnO_2 films deposited in presence of Triton X-100 is 345 $F g^{-1}$.

1. Introduction

Electrochemical capacitor, also known as supercapacitor, is a promising energy storage device for meeting the high-power electric market [1,2]. Several metal oxides and hydroxides for example, those of Ni, Co, V, and Mn, have been studied extensively for high power redox supercapacitor applications [3–5]. Among the metal oxides, manganese dioxide (MnO_2) is one of the promising materials due to its availability, cost-effectiveness and non-toxicity. There are several oxidation states, including Mn(0), Mn(II), Mn(III), Mn(IV), Mn(V), Mn(VI), and Mn(VII), for manganese oxides [6] hence they are often employed as the cathode materials in rechargeable batteries [7]. Recently, manganese oxides have been considered as a potential candidate for the electrode material of supercapacitors. MnO_2 can show excellent pseudo-capacitive behavior in aqueous solutions and conduct a specific capacitance of 160 $F g^{-1}$ [8,9]. However, this value is competitive with carbon supercapacitors, but falls far short of the 760 $F g^{-1}$ obtained with hydrous RuO_2 [10].

Beneficial effects of localizing heat through non-isothermal anode heating [16] on electro-kinetics, have led us to use a relatively new technique with more efficiency in energy conversion for the evaluation of electrodeposited MnO_2. Adsorption of surfactants at the electrode/solution interface appeared to be an attractive, simple methodology to improve the electrochemical processes at the substrate/electrolyte interface. Though researches have been carried out on surface active agents in electrochemistry for more than six to seven decades, just a few classes of materials have been well studied so far for a modification process in the presence of surfactants [11]. Employment of surfactants in this work is a natural outgrowth of numerous and valuable articles on surface active agents. As proposed by Rusling, surfactant layers are formed on the electrode surface with well-defined microstructures and these could serve as templates for the electrochemical reactivity [12]. The addition of organic surfactants in the precursor solution is extremely important due to their influence on morphological and structural properties of electrodeposits. Organic surfactants are commonly used in the electrodeposition to control the crystal shape and size, in order to produce high quality deposits. The role of the organic surfactants is to change the morphology of the deposit owing to their concentration-dependent specific activity during electrodeposition. The modified materials are expected to afford superior mass transport properties, through regular mesoporous networks as a result of modified growth on the surface of adsorbed organic surfactant layers [13].

In order to improve the supercapacitive properties, the surface of MnO_2 thin film should be modified. The aim of the present study is to electrochemically deposit MnO_2 in the presence of Triton X-100, which is a neutral surface active agent, in the electrolyte and to evaluate the electrodes for capacitor properties. The effect of

* Corresponding author. Tel.: +91 231 2609225; fax: +91 231 2692333.
E-mail address: l.chandrakant@yahoo.com (C.D. Lokhande).

0925-8388/$ – see front matter © 2011 Elsevier B.V. All rights reserved.
doi:10.1016/j.jallcom.2011.08.029

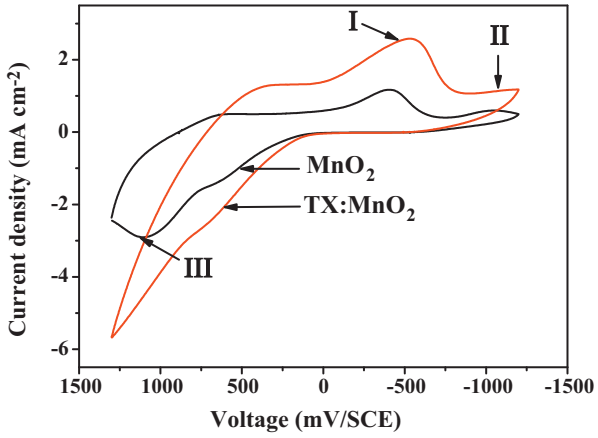

Fig. 1. Cyclic voltammograms for MnO_2 and TX:MnO_2 in the range of +1.3 to −1.2 V/SCE at the scan rate of 20 mV s^{-1}.

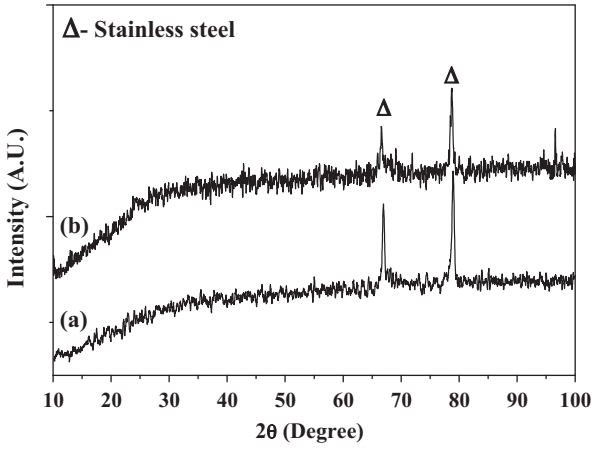

Fig. 2. The XRD patterns of (a) MnO_2 and (b) TX:MnO_2 thin films onto SS substrate.

surfactant (Triton X100) on structural, morphological, contact angle and supercapacitive properties of MnO_2 thin films are investigated.

2. Experimental details

Plating baths for MnO_2 and Triton X-100 assisted MnO_2 (TX:MnO_2) thin films were prepared with AR grade chemicals using double distilled water. The bath consisted of an aqueous solution of 0.1 M manganese sulphate ($MnSO_4{\cdot}4H_2O$) with 0.1 M citric acid {C (OH) (COOH) ($CH_2COOH)_2{\cdot}H_2O$} as a complexing agent, maintained at a pH of ~10.5 through the addition of 1 M sodium hydroxide (NaOH) solution. The concentration of organic surfactant (Triton X-100) was kept constant at 1 wt% in the final solution. The MnO_2 and TX-MnO_2 films are deposited onto a commercially pure stainless steel (SS) foil (SS 304) by potentiodynamic deposition. Before deposition, SS foil was polished with zero grade polish paper and then ultrasonically cleaned with double distilled water. Pure graphite was used as an anode. All deposition potentials were measured with respect to saturated calomel electrode (SCE) as a reference electrode. The depositions of MnO_2 and TX:MnO_2 were carried out potentiodynamically between the potential limits of +1.3 and −1.2 V/SCE at 20 mV s^{-1} scan rate using Potentiostat (EG and G-263A).

The structural characterization of the MnO_2 and TX:MnO_2 films was carried out using X-ray diffraction within the range 10–100° on computer controlled Philips PW-3710 using CrKα radiations (λ = 2.2897 Å). The surface morphological studies of films were carried out using FESEM (field emission scanning electron microscopy, Model: JSM-6701F, JEOL, Japan). The Fourier transform infrared (FTIR) spectra of the samples were collected using a 'Perkin Elmer, FTIR Spectrum one' unit. In order to study interaction between electrolyte and electrode surface contact angle measurement was carried out by Rame-hart USA equipment with CCD camera. The supercapacitor study was carried out using the 263A EG & G Princeton Applied Research Potentiostat forming an electrochemical cell comprising MnO_2/TX:MnO_2 film as a working electrode, platinum as a counter electrode and saturated calomel electrode (SCE) as a reference electrode in 1 M Na_2SO_4 electrolyte. Charge-discharge and impedance study was carried out using CHI 660D electrochemical workstation.

3. Results and discussion

3.1. Electrochemical deposition

Fig. 1 shows the typical cyclic voltammograms (CV) for MnO_2 and TX:MnO_2 in the range of +1.3 to −1.2 V/SCE at the scan rate of 20 mV s^{-1}. The cathodic peak (I) formed at −0.42 V/SCE may be due to the reduction of manganese at the surface of SS substrate. Deposition potential shifted toward negative region due to the strong complex formation in the solution.

$$2M(OH)^{2+} + 2e^- \rightarrow 2MnOOH + H_2\uparrow \text{ (Peak I)} \quad (-0.48\,V/SCE) \quad (1)$$

$$2MnOOH + 2e^- \rightarrow 2MnO_2 + H_2\uparrow \text{ (Peak II)} \quad (-1.25\,V/SCE) \quad (2)$$

Since, the bath is alkaline and complexed, the $Mn(OH)_2^+$ ions are formed which get attracted toward cathode at higher potentials than −1.1 V/SCE (Peak II) and reduction takes place by the formation of MnO_2. It is seen that, in reverse scan, there is a peak (III) (+1.0 V/SCE) which corresponds to the oxidation and dissolution of deposit into ions. The standard potentials are shown in bracket which is nearly the same. The slight variation in standard and observed potential is seen which may be due to substrate effect. The higher potential and alkaline medium assist the formation of MnO_2. As the adsorption of Mn^{2+} ions at the electrode surface precedes the electron-transfer process, it is inferred that Triton X-100 molecules favor this process, which results in higher anodic peak current for the oxidation of Mn^{2+} to MnO_2.

3.2. Structural characterization

Film crystallinity was analyzed using X-ray diffraction. The XRD patterns of MnO_2 and TX:MnO_2 on to the SS substrate are shown in Fig. 2. Both the XRD patterns do not show well-defined diffraction peaks other than SS substrate, indicating that MnO_2 films are amorphous. Thus, the data suggest that both samples are amorphous and Triton X-100 do not alter the amorphous nature of MnO_2. The obtained amorphous phase is feasible for supercapacitor application, since the protons can easily permeate through the bulk of the amorphous MnO_2 electrode materials and whole amount of electrode is utilized for energy storage [14].

3.3. Surface morphological studies

Many investigations have shown that rechargeability, current efficiency and stability depend significantly on the electrode morphology. Surfactants strongly affect the morphology and crystal growth in association with a promotion of nucleation and current distribution [13]. In this regard, the structure of products is controlled through a balance of thermodynamic and kinetic forces within different inorganic, organics as well as inorganic/organic interactions [15]. The SEM images of MnO_2 and TX:MnO_2 are shown in Fig. 3(a and b), respectively. The morphologies showed that the substrate is well covered with MnO_2 nanoparticles. From the Fig. 3(a), one can see the spherical grain morphology of MnO_2 spread over whole surface with porous structure. It is seen that the surface of TX:MnO_2 appears more uniform, rough, and porous, with smaller particles, suggesting a higher surface area than the smoother surface of MnO_2. Devaraj and Munichandraiah [16] prepared Triton X-100 assisted MnO_2 thin films and reported that due to addition of triton X-100 the surface of MnO_2 becomes porous and rough

3.4. FTIR studies

The FTIR absorption spectra of MnO_2 and TX:MnO_2 samples in the range 4000–400 cm^{-1} are shown in Fig. 4(a and b). The

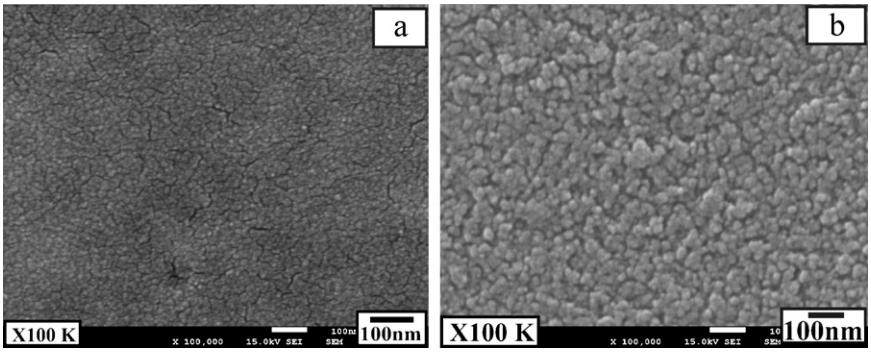

Fig. 3. Scanning electron micrographs of (a) MnO_2 and (b) TX:MnO_2 thin films at ×100k magnification.

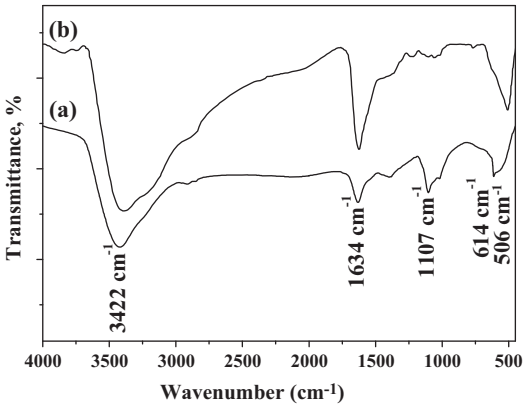

Fig. 4. FTIR spectra of (a) MnO_2 and (b) TX:MnO_2 thin films.

strong bands around at 614 cm^{-1} and 506 cm^{-1} are associated with the characteristic vibrational mode of Mn–O lattice [17]. The absorption peaks at around 1634 and 1107 cm^{-1} are assigned to –OH bending vibrations combined with Mn atoms [18]. The sharp absorption band at 3422 cm^{-1} is attributed to the –OH stretching vibrations. Shoulder of the 3422 cm^{-1} bond attributed to the hydrous nature of the MnO_2 material is highly intense in case of Triton X-100 assisted MnO_2. Thus results indicated that, as MnO_2 film contained hydroxide and Mn–O bonds, which indicates that formation of hydrous MnO_2 that may play important role in capacitive behavior [19]. From the FTIR study it is concluded that electrodeposited MnO_2 thin films are free from stray organic surfactant molecules.

3.5. Surface wettability test

Fig. 5(a and b) shows the measurement of water contact angles for MnO_2 and TX:MnO_2 thin films. From the images the contact angles for MnO_2 and TX:MnO_2 are found to be 45° and 10°, respectively. Decrease in contact angle for MnO_2 in presence of Triton X-100 is due to the hydroxyl bonds [20]. Triton X-100 molecules tend to be oriented with the phenyl ring toward the solution [15]. The presence of hydroxyl groups would strengthen the adsorbability toward the MnO_2 electrode surface, forming an adsorbed surfactant layer, rendering the surface more hydrophobic. Thus the triton X-100 contains hydroxyl groups due to which the surface becomes more hydrophilic [13] since there is cohesive force between the water droplet and hydroxyl groups. The contact angle factor is known to affect the wettability of a solid surface greatly. Generally, low water contact angle increases the electrochemical performance, where interfacial contact at electrolyte–electrode is important [21].

3.6. Supercapacitive study

3.6.1. Effect of Triton X-100 on supercapacitive properties of MnO_2 thin films

Cyclic voltammograms curves of MnO_2 and TX:MnO_2 electrodes in 1.0 M Na_2SO_4 are shown in Fig. 6(a and b). Cyclic voltammograms of both are rectangular in shape which is a fingerprint for capacitive behavior [22]. In addition to existence of double-layer capacitance, MnO_2 and TX:MnO_2 possesses pseudocapacitance due to Mn^{4+}/Mn^{3+} reversible redox reaction. This process is accompanied by reversible insertion/deinsertion of alkali cation (Na^+) or protons (H_3O^+) present in the electrolyte [23].

$$MnO_2 + M^+ + e^- \Leftrightarrow MnOOH \quad (3)$$

where M^+ is a cation. The supercapacitace increases from 210 to 278 $F\,g^{-1}$ due to Triton X-100 surfactant at 100 $mV\,s^{-1}$. The main reason for the enhancement in the supercapacitance is that the presence of TX-100 could strengthen the skeleton of the MnO_2 and prevents the capacity loss. Secondly, large surface area of the crystals decreases the solid-state diffusion path length of protons and electrons into and out of the bulk of MnO_2 films [24]. Therefore, more facilitated volume pulsations of MnO_2 during charge/discharge cycling, and consequently an increase of both discharge capacity and coulomb efficiency could be expected. Such features appear particularly important from the viewpoint of conductance, as these nanoparticles should allow a much better connection of MnO_2 with graphite, explaining the higher cycle performance of the corresponding cells [13].

3.6.2. Effect of scan rate

The voltammetric responses of TX:MnO_2 electrode at different scan rates is shown in Fig. 7. The effect of the scan rate from 5

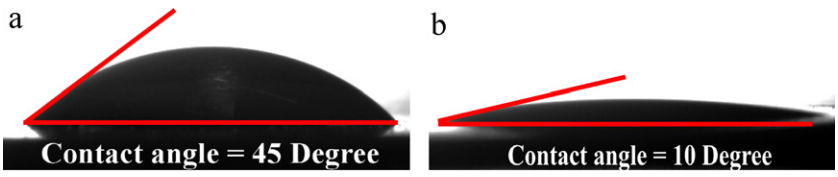

Fig. 5. Contact angle measurements of (a) MnO_2 and (b) TX:MnO_2 thin films.

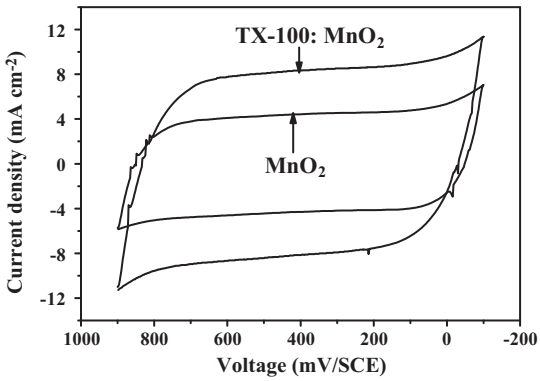

Fig. 6. Cyclic voltammograms of (a) MnO_2 and (b) TX:MnO_2 thin films in 1 M Na_2SO_4 electrolyte at 100 mV s^{-1}.

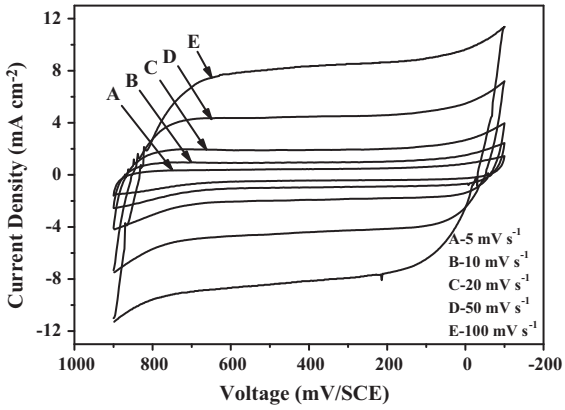

Fig. 7. Cyclic voltammograms of TX:MnO_2 thin film at different scanning rates in 1 M Na_2SO_4 electrolyte.

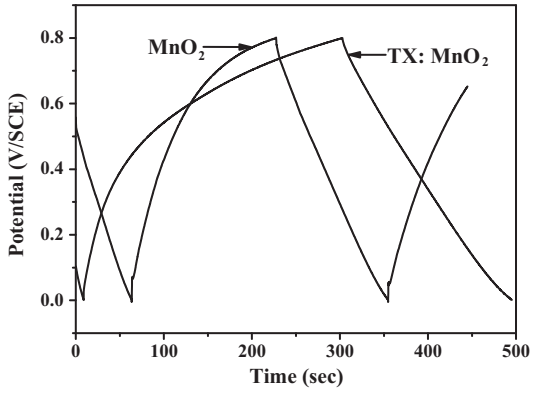

Fig. 8. Galvanostatic charge–discharge curves of MnO_2 and TX:MnO_2 thin film at 2 mA cm^{-2} in 1 M Na_2SO_4 electrolyte.

to 100 mV s^{-1} on supercapacitance of MnO_2 electrode is studied in 1.0 M Na_2SO_4 in voltage range of −0.1 to 0.9 V/SCE. There is a linear increase in voltammetric current density with an increase in scan rate, suggesting capacitive behavior of the electrodes [25]. The decrease in capacitance with the scan rate is attributed to the presence of inner active sites, which cannot precede the redox transitions completely at higher scan rate of CV, probably due to the diffusion effect of proton within the electrode. Maximum capacitance obtained for hydrous MnO_2 at lower scan rate (5 mV s^{-1}) is 345 F g^{-1}.

Table 1
Values of specific energy, specific power and coulomb efficiency of MnO_2 and TX:MnO_2 thin films.

Name	Specific energy (Wh kg^{-1})	Specific power (W kg^{-1})	Coulomb efficiency, η (%)
MnO_2	2.3	0.5×10^3	91
TX:MnO_2	3.4	0.6×10^3	93

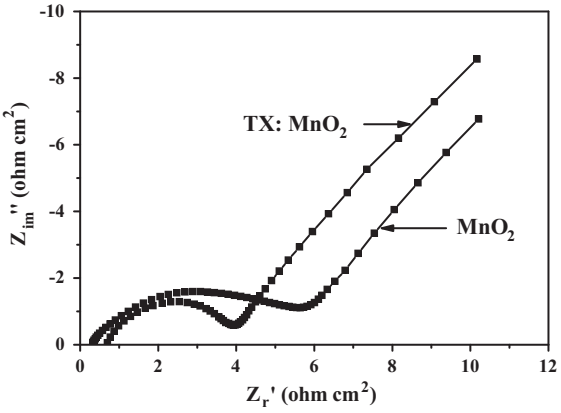

Fig. 9. Nyquist plots obtained for MnO_2 and TX:MnO_2 electrode at 0.8 V/SCE in 1 M Na_2SO_4 electrolyte.

3.6.3. Galvanostatic charge–discharge studies

MnO_2 and TX:MnO_2 electrodes were subjected to galvanostatic charge–discharge cycling between 0 and 0.8 V/SCE in aqueous 1.0 M Na_2SO_4 electrolyte at 2 mA cm^{-2} current density. The variation of potential during the cycle with time of cycling is shown in Fig. 8. There is a linear variation of potential during both charging and discharging processes. The linear variation of potential during charging and discharging processes is another criterion for capacitance behavior of material in addition to exhibiting rectangular voltammograms [22]. The durations of charge and discharge are nearly equal, implying high reversibility. The value of specific energy, specific power and coulomb efficiency for MnO_2 and TX:MnO_2 are listed in Table 1.

3.6.4. Electrochemical impedance analysis

Nyquist plots of ac impedance spectra of MnO_2 and TX:MnO_2 are presented in Fig. 9. The Nyquist plot consists of a high-frequency intercept on the real axis corresponding to the electrolyte resistance, a semicircle corresponding to a parallel combination of charge-transfer resistance (R_{ct}) and double-layer capacitance (C_{dl}), and finally a linear region at low-frequency range. From the Nyquist plot the electrolyte resistance is 0.6 Ω as seen from the intercept on the real axis. It was found that R_{ct} of 3.9 Ω cm^{-2} for MnO_2 in presence of Triton X-100 is smaller than that of 7 Ω cm^{-2} for MnO_2, this implies that the cation insertion/extraction process into/from TX:MnO_2 lattice is more facile than in the case of MnO_2. It is inferred that TX:MnO_2 is a better capacitive material in comparison with MnO_2. The results obtained here are in good agreement with earlier reported results [16].

4. Conclusions

Electrochemically deposited TX:MnO_2 thin films yields superior capacitive properties than plain MnO_2. The addition of triton X-100 does not alter the amorphous nature of MnO_2 thin films. FTIR studies revealed the formation of hydrous MnO_2 thin films. Due to addition of triton X-100, the MnO_2 film becomes superhydrophilic from hydrophilic. The supercapacitance of TX:MnO_2 decreased with increase in scan rate. Smaller particle size, greater

porosity, higher specific surface area, and higher efficiency of utilization of TX:MnO_2 in relation to MnO_2 are the factors responsible for obtaining higher specific capacitance. A specific capacitance of 345 F g^{-1} for TX:MnO_2 is obtained in the present study. The specific energy, specific power and coulomb efficiency are also increased due to Triton X-100. Thus, it is inferred that TX:MnO_2 is a better capacitive material in comparison with MnO_2.

Acknowledgements

One of the authors Prof. C. D. Lokhande is grateful to All India Council for Technical Education, New Delhi for financial support through scheme no. F. No.: 8023/BOR/RID/RPS-165/2009-10. Authors are also grateful to the Council for Scientific and Industrial Research (CSIR), New Delhi (INDIA) for financial support through the scheme no. 03(1165)/10/EMR-II.

References

[1] B.E. Conway, V. Briss, J. Wojtowicz, J. Power Sources 66 (1997) 1.
[2] R. Kotz, M. Carlen, Electrochim. Acta 45 (2000) 2483.
[3] T.C. Liu, W.G. Pell, B.E. Conway, Electrochim. Acta 44 (1999) 2829.
[4] H.Y. Lee, J.B. Goodenough, J. Solid State Chem. 148 (1999) 81.
[5] V. Srinivasan, J.W. Weidner, J. Power Sources 108 (2002) 15.
[6] M. Pourbaix, Atlas of Electrochemical Equilibria in Aqueous Solutions, National Association of Corrosion Engineers, Houston, TX, 1966, p. 286.
[7] M.M. Doeff, A. Anapolsky, L. Edman, T.J. Richardson, L.C. De Jonghe, J. Electrochem. Soc. 148 (2001) A230.
[8] T. Brousse, M. Toupin, R. Dugas, L. Athouel, O. Crosnier, D. Belanger, J. Electrochem. Soc. 153 (2006) A2171.
[9] R.N. Ready, R.G. Ready, J. Power Sources 132 (2004) 315.
[10] J.P. Zheng, Electrochem. Solid State Lett. 2 (1999) 359.
[11] R. Vittal, H. Gomathi, J. Phys. Chem. B 106 (2002) 10135.
[12] J.F. Rusling, Colloids Surf. 81 (1997) 123.
[13] M. Ghaemi, L. Khosravi-Fard, J. Neshati, J. Power Sources 141 (2005) 340.
[14] V.D. Patake, C.D. Lokhande, Appl. Surf. Sci. 254 (2008) 2820.
[15] Y.Z. Khimyak, J. Klinowski, J. Mater. Chem. 10 (2000) 1847.
[16] S. Devaraj, N. Munichandraiah, J. Electrochem. Soc. 154 (2007) A901.
[17] C.M. Julien, M. Massot, C. Poinsignon, Spectrochim. Acta 60 (2004) 689.
[18] M. Ocana, Colloid Polym. Sci. 278 (2000) 443.
[19] W. Sugimoto, H. Iwata, Y. Murakami, Y. Takasu, J. Electrochem. Soc. 151 (2004) A1181.
[20] A.V. Rao, S.S. Latthe, D.Y. Nadargi, H. Hirashima, V. Ganesan, J. Colloid Interface Sci. 332 (2009) 484.
[21] R.S. Mane, J. Chang, D. Ham, B.N. Pawar, T. Ganesh, B.W. Cho, J.K. Lee, S.H. Han, Curr. Appl. Phys. 9 (2009) 87.
[22] Conway BE, Electrochemical Supercapacitors, Kluwer Academic Publishers/Plenum Press, New York, 1999, p. 1.
[23] M. Toupin, T. Brousse, D. Belanger, Chem. Mater. 16 (2004) 3184.
[24] S.C. Pang, M.A. Anderson, T.W. Chapman, J. Electrochem. Soc. 147 (2000) 444.
[25] J.N. Broughton, M.J. Brett, Electrochem. Solid State Lett. 5 (A2) (2002) 79.